Check for updates

Original Research

Advances in Structural Engineering

Advances in Structural Engineering
1–16
© The Author(s) 2020
Article reuse guidelines:
sagepub.com/journals-permissions
DOI: 10.1177/1369433220919079
journals.sagepub.com/home/ase
SAGE

Vibration control of suspension bridge due to vertical ground motions

Seyed Hossein Hosseini Lavasani, Hamed Alizadeh, Rouzbeh Doroudi and Peyman Homami

Abstract

Suspension bridges due to their long span can experience large displacement response under dynamic loading like earthquakes. Unlike other structures, their vertical vibration may make remarkable difficulty that a control strategy seems to be essential. Tuned mass damper is a passive control system that can be changed to active one by adding an external source producing the active control force called active tuned mass damper. Unlike passive systems, active ones need a controller system affecting the performance of them considerably. In this study, the efficiency of tuned mass damper and active tuned mass damper are investigated in the bridges. Two controllers, fuzzy type 2 and fuzzy type 1, are used to estimate control force of active tuned mass damper. Tuned mass damper's parameters are optimized under wide range of ground motions. Also, fuzzy type 2 and fuzzy type 1's parameters are optimized under the influence of three different conditions containing far-field and near-field ground motions and also combination of them. In addition, Lion Pride Optimization Algorithm is selected for optimizing section. Numerical analysis indicates that active tuned mass damper is more effective than tuned mass damper, and also active tuned mass damper does not make any instability matter of concern in active control systems. Furthermore, performance of fuzzy type 2 is better than fuzzy type 1.

Keywords

active tuned mass damper, fuzzy type 2 controller, Lion Pride Optimization Algorithm, suspension bridge, tuned mass damper, vertical vibration

Introduction

Long span of suspension bridge leads to their vulnerability under ambient vibration like wind loading and ground motions. Suspension bridges can vibrate in four lateral, torsional, longitudinal, and vertical modes (Huang et al., 2005) . Generally, its ultimate response under vertical component of ground motions consists of pure vertical mode; however, it will be intensified by the horizontal excitation of the anchor blocks (Abdel-Ghaffar and Rubin, 1983). In the last decades, vibration control of the structures like tall buildings and bridges has been one of the most interesting field for engineers.

Control systems are categorized to the distinct groups namely passive, active, semi-active, and hybrid. Tuned mass damper (TMD) is a kind of passive control system containing three main parameters namely mass ratio, damping ratio, and tuning frequency (Elias and Matsagar, 2017a). Usually, it is tuned to first mode of the structure to mitigate the vibration by the resonance (Debbarma and Das, 2016). A number of scholars have investigated the effectiveness and ability of TMDs on control of civil structures including bridges and buildings (Amini and Doroudi, 2010; Carpineto et al., 2010; Elias and Matsagar, 2017b, 2017c; Hossein Lavassani et al., 2020; Larsena et al., 1995; Matin et al., 2020; Nikkhoo et al., 2019; Pourzeynali and Esteki, 2009; Wang et al., 2014). These articles indicate the promising effect of TMDs to reduce structural response of bridges and buildings.

In spite of existing many spaced modes in suspension bridge, tuning TMD to one certain mode of the structure may not provide the acceptable performance under dynamic loading like ground motions which generally involve the several modes of the structure, so a changeable parameter seems to be indispensable. An external power source generating various force which controls the vibration of structure is a mutable feature that creates a new active control system called active

Department of Civil Engineering, Faculty of Engineering, Kharazmi University, Tehran, Iran

Corresponding author:
Seyed Hossein Hosseini Lavasani, Department of Civil Engineering, Faculty of Engineering, Kharazmi University, Tehran 15614, Iran.
Email: lavasani@khu.ac.ir

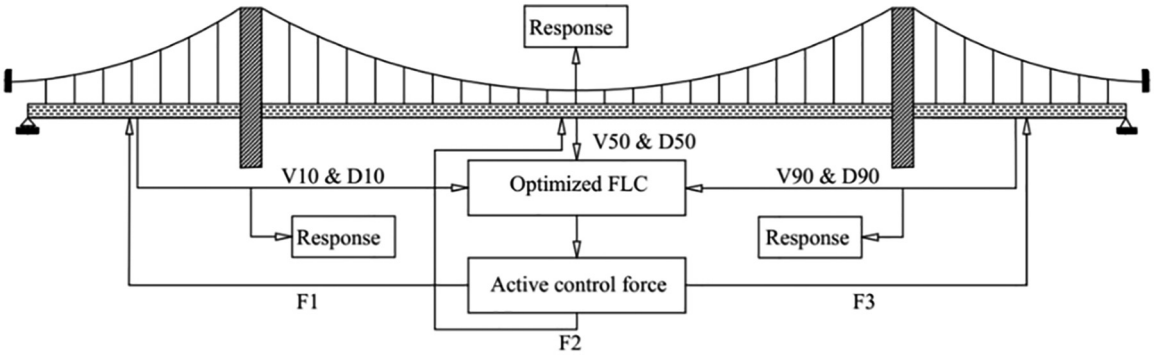


Figure 1. Close-loop control system.

tuned mass damper (ATMD). A number of scholars have investigated the effectiveness and ability of ATMD on control of bridges (Chen et al., 2011; Tanida, 2002; Wen and Sun, 2015).

ATMD needs a controller which can be optimized by whether classical or meta-heuristic optimization algorithm to achieve the best performance (Pourzeynali et al., 2007). Types 1 and 2 of the fuzzy algorithm (were introduced in 1965 and 1975, respectively) used in active control strategies and could be suitably optimized by meta-heuristic optimization algorithm (Castillo and Melin, 2008). Pourzeynali and Datta (2005) utilized fuzzy logic to control suspension bridge against flutter phenomenon. They used a semi-active tuned mass damper (STMD) which fuzzy logic was applied to select damping ratio of TMDs. The result showed that STMD was appropriate to mitigate response of the suspension bridge.

In this study, the performance of ATMD is investigated in the suspension bridges; also, it will be compared with the performance of TMD. Vincent Thomas suspension and Golden Gate bridges are chosen for case study, and their responses in the uncontrolled and controlled condition containing both TMD and ATMD systems under both near and far-field ground motions and combination of both of them are evaluated. Fuzzy type 2 and fuzzy type 1 are used as controllers for the active control system, and Lion Pride Optimization Algorithm (LPOA) as a meta-heuristic algorithm is utilized to optimize the membership functions (MFs) and rules of fuzzy logic controllers (FLCs). Also, the parameters of TMD will be optimized by mentioned algorithm. Figure 1 illustrates used control system.

Methodology

Motion equation

The ground motions excitation can be transmitted to the suspension bridge's structure by the support points, the anchorages, and piers. In this section, the response of the suspended structure is considered, and the equation of motion can be written using potential and kinetic energy and applying the Hamilton's energy principal as follows

$$[\mathrm{M}]\{\ddot{x}(t)\} + [C]\{\dot{x}(t)\} + [K]\{x(t)\} = -[M]\{r\}\ddot{x}_g(t) \quad (1)$$

where acceleration, velocity, and displacement response are represented by vectors $\{\ddot{x}(t)\}$, $\{\dot{x}(t)\}$, and $\{x(t)\}$, respectively. Also, $\{r\}$ is the location vector of ground accelerations $\{\ddot{x}_g(t)\}$. $[M]$, $[C]$, and $[K]$ are the mass, damping, and stiffness matrices of the bridge, respectively.

According to Figure 2, the suspended structure is divided to certain finite elements. Each element contains main cable, girder, and at least two hangers. The hangers are assumed to be inflexible, so assuming two nodes at the centerline of girder seems to be adequate. Each node includes two degrees of freedom namely vertical displacement and bending rotation. By assembling the structural property matrices of whole elements, two dimensional linear matrices of the suspended structure are obtained. In this regard, side spans divided to 11 elements while center one includes 28 elements. So, each of side spans includes square properties matrices with order 24 while this value for center span is 58. Because of that two hinged end of spans, vertical displacement will be eliminated at nodes 12, 13, 41, 42, and 51 which indicate the initial and end parts of spans. Also, there is not any interaction between the end and initial nodes of consecutive spans. Stiffness matrix is formed from three independent parts namely elastic stiffness of the girder (K_{ge}), elastic stiffness (K_{ce}), and gravity stiffness (K_{cg}) of the cable (Abdel-Ghaffar, 1980)

$$\left[k_{ge}\right]_e = \frac{E_g I_g}{L^3}\begin{bmatrix} 12 & -6L & -12 & -6L \\ -6L & 4L^2 & 6L & 2L^2 \\ -12 & 6L & 12 & 6L \\ -6L & 2L^2 & 6L & 4L^2 \end{bmatrix},$$

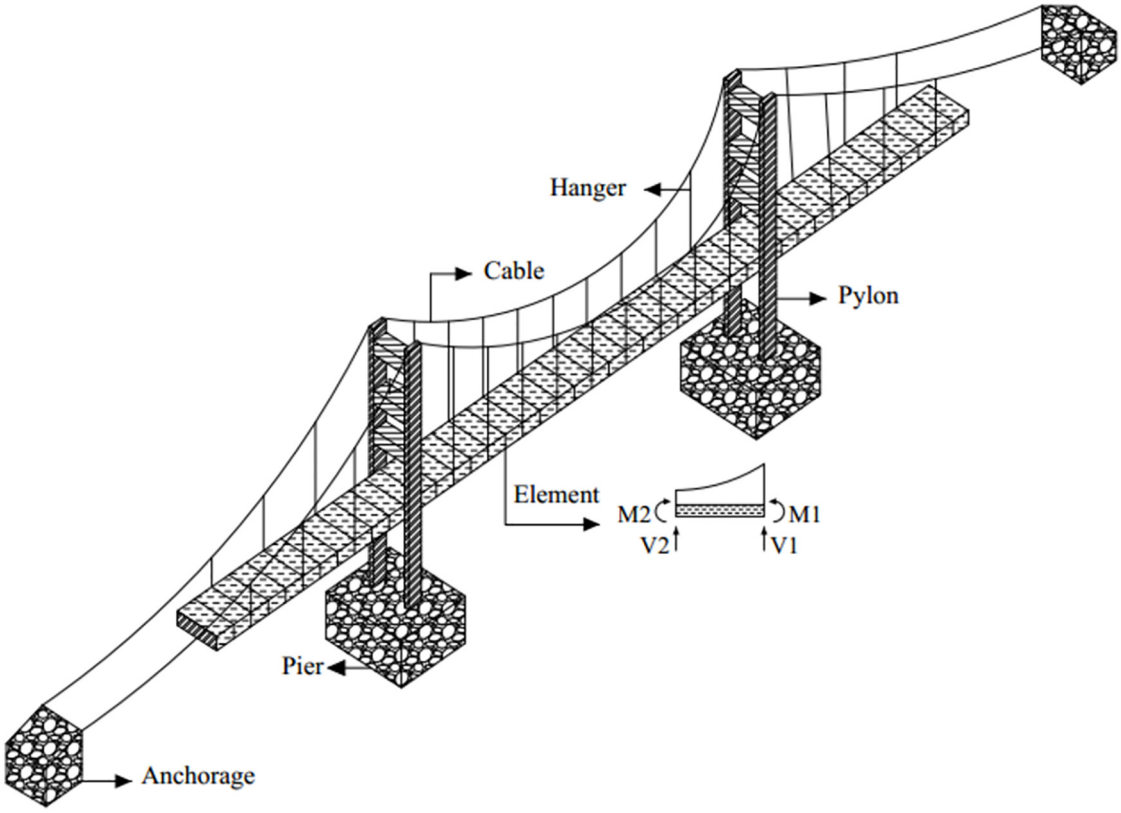


Figure 2. Finite element model of the whole bridge.

$$[k_{cg}] = \frac{-H_w}{30L}\begin{bmatrix} 36 & -3L & -36 & -3L \\ -3L & 4L^2 & 3L & -L^2 \\ -36 & 3L & 36 & 3L \\ -3L & -L^2 & 3L & 4L^2 \end{bmatrix} \tag{2}$$

$$[k_{ce}]_e = \frac{E_c A_c}{L_E} * \left(\sum_{i=1}^{3} \frac{W_d}{H_w}\left\{\hat{f}\right\}_{N_i}\right) * \left(\sum_{i=1}^{3} \frac{W_d}{H_w}\left\{\hat{f}\right\}_{N_i}^{T}\right).$$

$$\left\{\hat{f}\right\}^T = \left[\frac{L}{2}.\frac{-L^2}{12}.\frac{L}{2}.\frac{L^2}{12}\right] \tag{3}$$

Also, mass matrix is evaluated by the following matrix

$$[m_t]_e = \frac{m_t L}{420}\begin{bmatrix} 156 & -22L & 54 & 13L \\ -22L & 4L^2 & -13L & -3L^2 \\ 54 & -13L & 156 & 22L \\ 13L & -3L^2 & 22L & 4L^2 \end{bmatrix} \tag{4}$$

where L, L_E, A_C, and I_g are the span length, virtual length, cross section of the cable, and moment inertia of the girder, respectively. W_d and H_w are the Dead load of the whole suspended structure and Cable force. Also, E_g and E_c show the modulus of elasticity. In addition, Rayleigh method is utilized to evaluation the damping matrix (Clough and Penzien, 2010)

$$[C] = a_0[M] + a_1[K] \tag{5}$$

$$\frac{1}{2}\begin{bmatrix} \frac{1}{\omega_i} & \omega_i \\ \frac{1}{\omega_j} & \omega_j \end{bmatrix}\begin{Bmatrix} a_0 \\ a_1 \end{Bmatrix} = \begin{Bmatrix} \xi_i \\ \xi_j \end{Bmatrix} \tag{6}$$

Where ξ_i and ξ_j are the natural frequencies of the ith and jth modes of the bridge, where i and j are chosen as the first and 10th vibration modes of the bridge, respectively. Furthermore, ξ_i and ξ_j are equal to one percentage.

In order to decrease the volume of computation, the condensation process is utilized where the vertical degrees of freedom are considered as the master (m) while bending rotation degrees are slave ones. The related relation are as follows

$$x = \begin{Bmatrix} x_m \\ x_s \end{Bmatrix} \tag{7}$$

$$\begin{bmatrix} M_{mm} & M_{ms} \\ M_{sm} & M_{ss} \end{bmatrix}\begin{Bmatrix} \ddot{x}_m \\ \ddot{x}_s \end{Bmatrix} + \begin{bmatrix} K_{mm} & K_{ms} \\ K_{sm} & K_{ss} \end{bmatrix}\begin{Bmatrix} x_m \\ x_s \end{Bmatrix} = 0 \tag{8}$$

$$\tilde{K} = K_{mm} - K_{ms}K_{ss}^{-1}K_{sm} \tag{9}$$

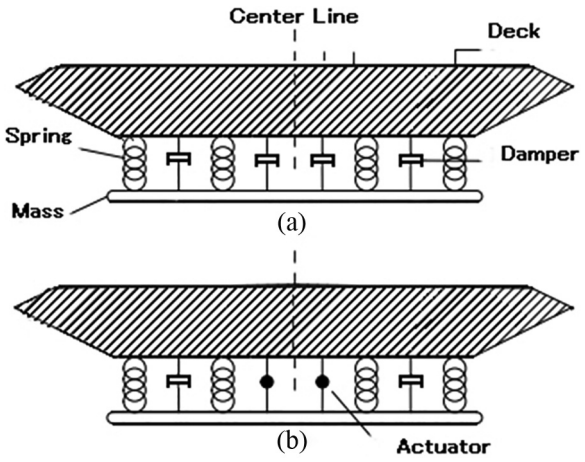


Figure 3. Cross section of the (a) bridge-TMD and (b) bridge-ATMD system.

$$\tilde{M} = M_{mm} - M_{ms} - M_{ms}K_{ss}^{-1}K_{sm} - K_{ms}K_{ss}^{-1}M_{sm} + K_{ms}K_{ss}^{-1}M_{ss}K_{ss}^{-1}M_{ss}K_{ss}^{-1}K_{sm} \quad (10)$$

In fact, the effects of the bending rotation are not eliminated and are considered in the $\tilde{K}$ and $\tilde{M}$ matrices.

ATMD and TMD

TMD is a passive control system including three main sectors namely mass, damper, and spring computable by following equation

$$k_T = m_T(\omega_N)^2 \quad (11)$$

$$C_T = 2\xi_T m_T \omega_N \quad (12)$$

where m_T and ω_N are the mass ratio and a certain mode of structure that TMD is tuned to them. Also, sub-indexes T and N denote the TMD and number of specified mode. Adding an actuator which imposes external force to TMD is defined as Active Tuned Mass Damper. Passive TMD is effective when one mode of the structure is dominant in the ultimate response like the first torsional mode in the flutter condition, but when the response is the combination of several modes like earthquake loading, the ATMD can provide better performance in comparison to TMD. On the other hand, TMD during dynamic loading does not cause instability of structures but ATMD may do this as a result of having external power. Therefore, this control force should be optimized in a manner that not only represents the maximum reduction of the response but also does not make any instability. Figure 3 illustrates the simplest attachment of the TMD and ATMD to the typical streamline deck. The springs and dampers can be distributed along the cross section of the bridge's deck in the passive system, and in active condition actuators also can be located between them.

The equation of motion with presence of ATMD can be written as follows

$$[M_s]\{\ddot{u}(t)\} + [C_s]\{\dot{u}(t)\} + [K_s]\{u(t)\} = -[M_s]\{r\}\ddot{u}_g(t) + [D]\{f\} \quad (13)$$

Sub-index s signifies the combined system of the bridge and ATMD. D is the location matrix of control force with order $n \times m$, and f is the control force vector with order $m \times 1$. Also, m denotes the used number of ATMDs. Due to assumption of elastic and linear model, the computation can be conducted comfortably in the state-space

$$\{\dot{Z}\}_{2n*1} = \begin{bmatrix} 0 & I \\ -M^{-1}K & -M^{-1}C \end{bmatrix}_{2(n+1)*2(n+1)} \{Z\}_{2(n+1)*1} + \begin{Bmatrix} 0_{(n+1)*1} \\ 1_{(n+1)*1} \end{Bmatrix}(-r)\ddot{u}_g(t), Z = \begin{Bmatrix} u(t) \\ \dot{u}(t) \end{Bmatrix} \quad (14)$$

where I is the identity matrix of order $n + m$, and [0] and {0} are the zero matrix and vector with order $n + m \times n + m$ and $n + m \times 1$, respectively. In addition, n denotes the total degrees of freedom and Z is the state-space vector. Ultimate response is computed by following relation

$$\{d\} = [C1]\{Z\}, [C1] = \begin{bmatrix} 1 & \dots & 1 & 0 & \dots & 0 \\ 0 & \dots & 0 & 0 & \dots & 0 \end{bmatrix}_{2*2(n+m)} \quad (15)$$

If an ATMD is placed at any node and the vertical degree of it locates at row i and column j through the structural matrices, the novel configuration of matrices are as follows

$$k_{ij}^{new} = k_{ij}^{old} + k_T, k_{i(n+1)} = -k_T, k_{(n+1)i} = -k_T, k_{(n+1)(n+1)} = k_T \quad (16)$$

where k represents the component of the stiffness matrix of the bridge. It should be noted that damping matrix is made in a similar manner. Also, for mass matrix

$$m_{ij}^{new} = m_{ij}^{old} + m_T, m_{(n+1)(n+1)} = m_T \quad (17)$$

where m shows the component of the mass matrix. The equation can be extended easily for more ATMDs.

Fuzzy logic controller

Fuzzy logic was introduced by Lotfi A. Zadeh. Fuzzy control applies expert knowledge instead of differential equations to define a system. It is a method using fuzzy information to estimate appropriate control actions and is used in complex systems. Designing of FLC contains the selection of the input, output variables, MF, and fuzzy rules. Because of its simplicity, nonlinear mapping ability, and robustness and validity, the FLC has been used to estimate the proper control force in many structural control applications.

In structural control, researchers utilize a combination of acceleration, velocity, and displacement or individually as inputs and control force as output for FLC. Even though, many researches have used type 1 FLC to better performance of structures against dynamic loads, there are some limitations to control the vibrations using these controllers. For example, type 1 FLCs cannot describe uncertainty very well (Bathaei et al., 2017). Nonetheless, uncertainty can be handled by type 2 FLC more than type 1 FLC (Castillo and Melin, 2008). Fuzzy control is based on if-then rules connecting the input information to generate appropriate output. It has three steps: (1) fuzzification, which the crisp value of the input information is transformed to a fuzzy linguistic value utilizing MFs; (2) decision making that uses "if-then" rules to conclude the linguistic value of the output; and (3) defuzzification, where the fuzzy output is transformed to a crisp value (Ross, 2010; Siddique and Adeli, 2013). Hence, designing proper FLC has two parts called (a) designing MFs and (2) designing fuzzy rule.

Design of MFs. All information contained in a fuzzy set is represented by its MF. MF categorizes the element in the set, whether it is discrete or continuous. Graphical representations including different shapes form the MFs. One of very important criteria for having successful implementation of FLC is the shape of MF. There are different shapes for MFs represented by mathematical formulations. Triangle MF of type 1 is one of the applicable and smooth MFs. The triangle MF is described by three parameters $\{a, b, c\}$

$$\mu_A(x) = \begin{cases} \dfrac{x-a}{b-a} & a \leqslant x \leqslant b \\ \dfrac{c-x}{c-b} & b \leqslant x \leqslant c \\ 0 & a < x \text{ or } x > c \end{cases} \tag{18}$$

where a is the left position, c is the right position, and b is the peak. The left width is the length of the interval from the peak value to the point to the left where the membership value is zero, and the right width is the length of the interval from the peak value to the point to the right where the membership value is zero. The left and peak position of the next MF is the same as the peak and right position of the previous MF so that MFs perform better for FLC (Siddique and Adeli, 2013).

The triangle MF of type 2 is mathematically defined on interval [0, 1] as follows (Ling and Zhang, 2011)

$$f_x(u) = \begin{cases} \dfrac{h_A(u-a)}{c-a} & a < u \leqslant c \\ \dfrac{h_A(u-b)}{c-b} & c < u \leqslant b \\ 0 & 0 \leqslant u < c \text{ or } 1 \geqslant u > b. \end{cases} \tag{19}$$

where $0 \leqslant a \leqslant c \leqslant b \leqslant 1$ and $h_A = Sup(f_x(\theta)) = f_a(c) \in [0, 1]$. The a, b, c, and h_a are parameters of type 2 FLC. In addition, triangle MF of type 2 has two bounds. First one is upper bound and the other is lower bound.

In this study, triangular MF is utilized as MFs for input and output variables, respectively. In addition, velocity and displacement are selected as input variables and control force is chosen as output variable for ATMD. FLC is designed with two input variables, each having three triangular MFs and one output variable with five triangular MFs. Triangular MFs for input (displacement, velocity) containing parameters a, b, and c and output (control force) are defined on the interval $[-1, 1]$.

Design of fuzzy rule. The achievement and performance of an FLC depends mostly on the rule base. The rule base is represented by a sequence if-then rules based (fuzzy conditional statements) on human being's knowledge or experience. On the other hand, the rule set forms the relationships between output and input MFs. The numbers of rules depend on the number of input MFs. For instant, if an FLC have two inputs and each of them includes three MFs, the fuzzy rule base will have nine if-then rules to cover all the rules between input and outputs variables. The definitions of the fuzzy variables of input MF (displacement, velocity) are as follows: N = Negative, Z = Zero, and P = Positive. The definitions of the fuzzy variables of the output MF (control force) are as follows: NL = Negative Large, NS = Negative Small, ZE = Zero, PS = Positive Small, and PL = Positive Large.

The number of rules in an FLC increases with the number of input/output variables and linguistic terms for each variable. Therefore, by growing input/output variables, it would be difficult to extract appropriate fuzzy rules. Refining and tuning fuzzy rules are very effective to solve the problem. Representation of the linguistic value of the output variable by integer values

Table 1. Designed variables.

Designed variables	Definition	Range
1, 2, 3	a_{t1}, b_{t1}, c_{t1} which are the parameters of triangle membership functions of type 1 for input (displacement)	real number on the interval [−1, 1]
4, 5, 6	d_{t1}, e_{t1}, f_{t1} which are the parameters of triangle membership functions of type 1 for input (velocity)	real number on the interval [−1, 1]
7	linguistic value of the output variable	integer number from 1 to 5
8, 9, 10, 11, 12, 13	a_{t2}, b_{t2}, c_{t2} which are the parameters of triangle membership functions of type 2 including upper and lower bound for input (displacement)	real number on the interval [−1, 1]
14	h_{A1} the parameter of type 2 for input (displacement)	real number on the interval [0, 1]
15, 16, 17, 18, 19, 20	d_{t2}, e_{t2}, f_{t2} which are the parameters of triangle membership functions type 2 including upper and lower bound for input (velocity)	real number on the interval [−1, 1]
21	h_{A2} the parameter of type 2 for output (velocity)	real number on the interval [0, 1]
22	μ is the TMD mass to the mass of the main structure	real number on the interval [0.01, 0.05]
23	f_d is natural frequency	real number on the interval [0.8, 1.2]
24	ξ_d is damping ratio	real number on the interval [0.02, 0.2]

TMD: tuned mass damper.

is one worthwhile approach to refine and tune fuzzy rules (Siddique and Adeli, 2013). Since the number of MFs for output variable is five, the linguistic value of the output variable is one to five for this study.

Optimal model

One of the most important considerations in designing fuzzy systems is selecting MFs and a relevant fuzzy rule base. It has been done either by a trial and error or by human experts. Therefore, the fuzzy systems created by this approach do not have proper result to find out the best solution for a complicated problem.

Tuning parameters of TMD is very significant to enhance performance of each one of control systems working with TMD (passive TMD, ATMD).

An optimization approach solves this intricate issue by formulating parameters of FLC and TMD as a search problem in a high-dimensional space where each point in the space illustrates parameters of MF, rule base set and TMD's parameters.

In this study, the minimization of the peak displacement value of the all nodes of a suspension bridge equipped by TMDs and ATMDs is subject to some earthquake excitations considered as the objective function which is calculated as follows

$$Minimize\ Z = \frac{(J_2 - J_1)}{(J_1)} \tag{20}$$

where J_1 is root-mean-square deviation (RMSD) of maximum uncontrolled displacement of all nodes which is calculated by solving equation (13) without applying control forces.

J_2 is RMSD of maximum controlled displacement of all nodes which is calculated by solving equation (13) by using TMDs and ATMDs.

Control systems are performed by optimal FLC which depends on MFs and fuzzy rule. Hence, parameters of MFs, fuzzy rule, and TMD's parameters are considered as designed variables. Table 1 shows designed variables.

Energy dissipated

Energy dissipated due to installation of control devices is a very important criterion to verify the effectiveness of control system. In this study, four different criteria including input energy, damping energy, strain energy, and kinetic energy are selected to investigate. The formulation and definition of them are as follows (Elias, 2018):

E_d is defined as the damping energy per mass of the bridge and dampers and calculated as follows

$$E_d = \frac{1}{(M_t)} \sum_{0}^{t_k} \begin{Bmatrix} \{dX\}_{N\times 1} \\ \{dx\}_{n\times 1} \end{Bmatrix}^T \begin{bmatrix} [C_N]_{N\times N} + [c_n]_{N\times N} & -[c_n]_{N\times N} \\ -[c_n]_{n\times N} & [c_n]_{n\times n} \end{bmatrix} \begin{Bmatrix} \{\dot{X}_i\}_{N\times 1} \\ \{\dot{x}_i\}_{n\times 1} \end{Bmatrix} \tag{21}$$

where $\{dX_i\}_{t_d} = \{X_i\}_{t_d} - \{X_i\}_{t_d}$ and $\{dx_i\}_{t_d} = \{x_i\}_{t_d} - \{x_i\}_{t_d}$, and t_k and t_d are duration and time step of earthquake respectively. N is degree freedom of structure and n is number of installed dampers and M_t is total mass of the bridge.

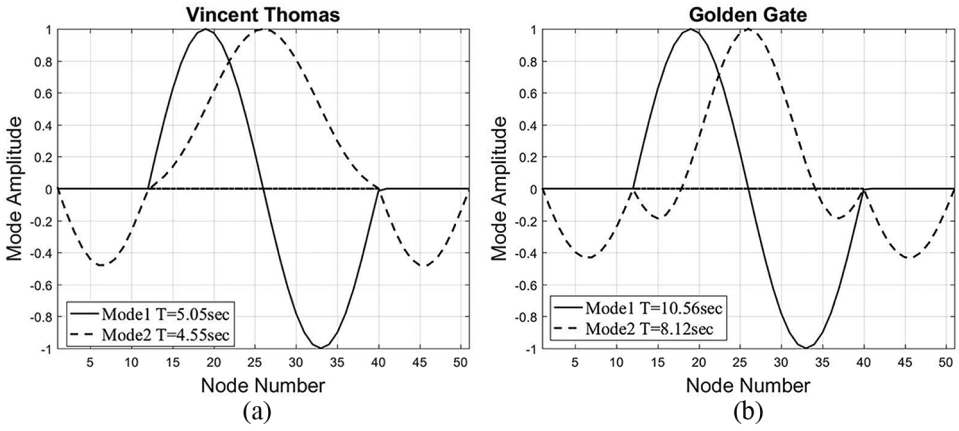


Figure 4. First symmetrical and unsymmetrical mode shapes.

Table 2. Verification of the computed frequencies.

No.		1	2	3	4	5	6	7	8	9
Frequency (rad/s)	Vincent Thomas	1.23	1.38	2.16	2.17	2.9	3.42	5	6.83	6.83
	Golden Gate	0.59	0.77	0.97	1.13	1.27	1.59	1.79	2.11	2.61
Frequency computed by Abdel-Ghaffar (rad/s)	Vincent Thomas	1.24	1.38	2.18	2.18	2.88	3.46	5.07	6.92	6.92
	Golden Gate	0.6	0.77	0.92	1.14	1.28	1.60	1.8	2.11	2.61

Lion Pride Optimization Algorithm

In this article, LPOA is utilized to optimize the parameters of TMD and FLC. LPOA is a search heuristic based on effect of influence of the natural collective behavior of lions in their life, and each agent is considered as a lion that was originally introduced by Kaveh and Mahjoubi (2018).

The algorithm has two distinct types of search agents with different types of specific rules. In addition, they are divided into sub-groups, namely prides consisting of females and males to probe search space independently. Hence, the cumulative knowledge achieved by each pride's member is different from members of the other prides. The algorithm has six steps: (1) *Social groups*, forming search agents containing lions and lionesses which explore the search space systematically. (2) *Hunting*, sorting lionesses according to their fitness. Then, dividing them into three groups in order to liken other members of divided group to the beast fitness members. (iii) *Excursion*, it is used to probe search space to find out new solutions. (iv) *Mating*, to generate next generation by mating lions and lionesses to find out new solution. (v) *Intragroup interaction*, sorts all new male and old male. Omitting the weakest one to improve the fitness of group. (vi) *Migration*, sorting all new female and old female. Omitting the weakest one to improve the fitness of group. The suitable balance between exploration and exploitation is formed by using six steps. More details of LPOA have been given by Kaveh and Mahjoubi (2018).

Numerical analysis

The Vincent Thomas and Golden Gate suspension bridges located in Los Angeles and San Francisco as the short and long ones, respectively, are selected for case studies. The bridges have three spans (that side ones are symmetric) including truss-type stiffening two hinged girders. Initial two mode shapes and first nine frequencies are demonstrated in Figure 4 and Table 2. Also, the supplementary data of bridge is provided in Table 3.

LPOA is utilized to optimize FLC and TMD's parameters. Fuzzy MFs (triangle) for inputs are tuned, and fuzzy rules are extracted in order to find out appropriate control force for ATMD to mitigate the peak seismic response of the bridge (maximum displacement). Fuzzy logic containing MFs, rule base, and LPOA are coded in MATLAB environment. Eight historical earthquake records are chosen to realize optimal parameters including FLC and TMD from a complete set of ground motions covering wide range of various earthquakes which are summarized in Table 4. Ground motion records are divided into three parts which the suspension bridge are subjected to them. First group includes four near-field earthquakes, the second one

Table 3. Structural and geometrical information of the Vincent Thomas and Golden Gate bridges.

Parameter	Vincent Thomas		Golden Gate	
	Side	Center	Side	Center
Length (m)	155	460	343	1281
Total dead load of the bridge (kg/m)	5347	5347	17,188	17,039
Elasticity modulus of the stiffening structure (MN/m^2)	200,027		200,027	
Moment inertia of the stiffening structure for side spans (m^4)	0.3749	0.3729	1.6782	2.5893
Horizontal tension of cable (kN)	30,038	30,038	237,914	
Elasticity modulus of the cable (MN/m^2)	186,000		200,027	
Cross section area of one cable (m^2)	0.0781		0.53	
Virtual length of cable (m)	281	494	470	1408

Table 4. Selected earthquake's data.

Type	No.	Earthquake	Station	Year	Distance to fault (m)	Magnitude	PGA (g)	Fault mechanism
NF	1	Bam	Bam	2003	0.05	6.6	0.97	Strike slip
	2	Northridge	Rinaldi	1994	7.1	6.7	0.852	Reverse
	3	Landers	Lucern	1992	2.19	7.28	0.823	Strike slip
	4	Tabas	Tabas	1978	1.79	7.35	0.641	Reverse
	5	Imperial valley	El Centro #07	1979	0.56	6.53	0.544	Strike slip
	6	Kobe	Kobe University	1995	0.9	6.9	0.452	Strike slip
	7	Chi-Chi	TCU129	1999	1.83	7.62	0.342	Reverse oblique
	8	Northridge	Tarzana	1978	16.7	6.69	1	—
	9	Erzincan	Erzincan	1992	2	6.7	0.248	Strike slip
	10	Kocaeli	Izmit	1999	3.62	7.51	0.145	Strike slip
FF	11	Chi-Chi	TCU045	1999	26	7.62	0.356	Reverse oblique
	12	Imperial valley	El Centro #09	1940	213	6.09	0.18	Strike slip
	13	Duzci	Bolu	1999	17.6	7.1	0.203	—
	14	Cape Mendocino	Petrolia	1992	35.1	7.01	0.15	Reverse
	15	Kobe	Kakogawa	1995	22.5	6.9	0.171	Strike slip
	16	Northridge	Moorpark	1994	26.4	6.69	0.14	Reverse
	17	Landers	Cool Water	1992	19.74	7.28	0.17	Strike slip
	18	San Fernando	Castic-Old Ridge	1971	19.33	6.61	0.167	Reverse
	19	Kocaeli	Faith	1999	53.34	7.51	0.133	Strike slip
	20	Park field	Temblo Pre	1969	15.96	6	0.13	Strike slip

PGA: peak ground acceleration; NF: near-field ground motions; FF: far-field ground motions.

contains four far-field earthquakes, and the last one includes two near and far-field earthquakes. Hence, three different optimal models of FLC are selected to generate control force of ATMD which they are sensitive to far-field (F) and near-field (N) earthquakes, or combination (NF) of them.

In this study, the specifications of TMD are optimized in account to structural properties of each span. This procedure represents the lighter and more economical devices. In tuning optimization phase, instead of the finding optimum mode, first mode of bridges is selected as the base mode and then frequency ratio as a creative parameter should be optimized. The ground motions records are imposed to the suspended structure continuously to achieve the optimum values of TMD's parameters. In order to have the comparative study, the computed optimum values are used in the ATMD system. Table 5 shows optimal parameters of TMD.

Table 5 summarizes triangular MFs for the inputs (displacement and velocity) include fuzzy membership parameters for type 1 and type 2 after training and tuning by LPOA. The left and right poisons, and the peak value of MFs are -1.00, 0.25, 1.00, -0.76, 0.35, 0.76 and -0.99, 0.40, 0.99, -1.00, 0.45, 1.00 and -1.00, 0.38, 1.00, -1.00, 0.35, 1.00 for ATMD in different optimal type 1 FLCs including far field, near field and near-far field, respectively. Furthermore, parameters of type 2 controllers which are optimized under far-field earthquakes are -0.98, -0.46, -0.93, 0.94, 0.46, 0.99, 1, 1 for upper bound and -0.99, -0.75, -0.88, 0.88, 0.75, 0.99, 0.81, 0.86 for lower bound.

The fuzzy rule base includes nine if-then rules for type 1 far-field control system represented as follows:

Table 5. The parameters of membership functions of fuzzy controllers and the rule base for fuzzy logic and optimal parameters of TMD.

Control system									
Type 1 far-field		a_{t1}	b_{t1}	c_{t1}	d_{t1}	e_{t1}		f_{t1}	
		−1.00	0.25	1	−0.76	0.35		0.76	
Fuzzy rule			Displacement	Velocity					
					N	Z	P		
				N	NL	NS	NS		
				Z	NS	ZE	PS		
				P	NS	PS	PL		
Type 1 near-field		a_{t1}	b_{t1}	c_{t1}	d_{t1}	e_{t1}		f_{t1}	
		−0.99	0.40	0.99	−1.00	0.45		1.00	
Fuzzy rule			Displacement	Velocity					
					N	Z	P		
				N	NL	NS	NS		
				Z	NS	ZE	PS		
				P	NS	PS	PL		
Type 1 near-far field		a_{t1}	b_{t1}	c_{t1}	d_{t1}	e_{t1}		f_{t1}	
		−1.00	0.38	1.00	−1.00	0.35		1.00	
Fuzzy rule			Displacement	Velocity					
					N	Z	P		
				N	NL	NS	NS		
				Z	NS	ZE	PS		
				P	NS	PS	PL		
Type 2 far-field		a_{t2}	b_{t2}	c_{t2}	d_{t2}	e_{t2}	f_{t2}	h_{A1}	h_{A2}
	Upper	−0.95	−0.10	0.95	−0.92	0.15	0.92	1	1
	Lower	−0.91	−0.15	0.91	−0.80	0.20	0.80	0.83	0.81
Fuzzy rule			Displacement	Velocity					
					N	Z	P		
				N	NL	NS	NS		
				Z	NS	ZE	PS		
				P	NS	PS	PL		
Type 2 near-field		a_{t2}	b_{t2}	c_{t2}	d_{t2}	e_{t2}	f_{t2}	h_{A1}	h_{A2}
	Upper	−0.98	−0.16	0.98	−0.99	0.06	0.99	1	1
	Lower	−0.95	−0.25	0.95	−0.88	0.15	0.88	0.81	0.86
Fuzzy rule			Displacement	Velocity					
					N	Z	P		
				N	NL	NS	NS		
				Z	NS	ZE	PS		
				P	NS	PS	PL		
Type 2 near-far field		a_{t2}	b_{t2}	c_{t2}	d_{t2}	e_{t2}	f_{t2}	h_{A1}	h_{A2}
	Upper	−0.93	−0.10	0.93	−0.90	0.05	0.90	1	1
	Lower	−0.92	−0.20	0.92	−0.84	0.15	0.84	0.83	0.82
Fuzzy rule			Displacement	Velocity					
					N	Z	P		
				N	NL	NS	NS		
				Z	NS	ZE	PS		
				P	NS	PS	PL		

Bridge	Mass ratio		Damping ratio		Frequency ratio		Host nodes	
	Side	Center	Side	Center	Side	Center	Side	Center
Vincent Thomas	15	8	30	30	1.5	0.88	6.46	26
Golden Gate	15	8	30	30	1.5	1.5	6.46	26

TMD: tuned mass damper.

1. If input MF (displacement) is N and input MF (velocity) is N, then output MF (control force) is NL

⋮

9. If input MF (displacement) is P and input MF (velocity) is P, then output MF (control force) is PL

Furthermore, for type 2 far-field system, the rules are represented as follows:

1. If input MF (displacement) is N and input MF (velocity) is N, then output MF (control force) is NL

⋮

9. If input MF (displacement) is P and input MF (velocity) is P, then output MF (control force) is PL

Table 5 demonstrates other rule base and parameters of MF of different control systems.

Robustness of designed control systems

The suspension bridges equipped with different optimal control systems are subjected to the set of mentioned earthquakes in order to figure out the robustness of the optimal control systems. Maximum controlled and uncontrolled displacement of the three spans of the considered suspension bridges for each earthquake are illustrated in Figures 5 and 6. Because first and third spans are symmetric, therefore, both responses are equal.

ATMD and TMD systems reduce the displacement response of the bridge successfully. Also, ATMDs optimized by three different conditions illustrate lower responses into TMDs. Even though optimized ATMD will represent appropriate performance under any circumstance, the efficiency of three conditions are different. According to Figures 5 and 6, the result of uncontrolled responses in comparison to controlled responses are as follows: controlled responses of first and third spans of Vincent Thomas suspension bridge in comparison to uncontrolled responses for all earthquakes reduce 24.66%, 40.19%, 32.43%, 32.64%, 46.99%, 62.05%, and 60.33% for TMD, type 1 far field, type 1 near field, type 1 far-near field, type 2 far field, type 2 near field, and type 2 far-near field, respectively. In addition, for second span of Vincent Thomas suspension bridge, seismic responses reduce 20.34%, 41.01%, 28.75%, 29.34%, 46.03%, 62.92%, and 61.07% for TMD, type 1 far field, type 1 near field, type 1 far-near field, type 2 far field, type 2 near field, and type 2 far-near field, respectively.

Furthermore, reduction of controlled responses of first and third spans of Golden Gate suspension bridge in comparison to uncontrolled responses for all earthquakes are 18.67%, 36.25%, 51.04%, 49.38%, 46.13%, 61.70%, and 60.22% for TMD, type 1 far field, type 1 near field, type 1 far-near field, type 2 far field, type 2 near field, and type 2 far-near field, respectively. In addition, for second span of Golden Gate suspension bridge, seismic responses reduce 18.82%, 37.27%, 50.14%, 48.65%, 47.23%, 60.78%, and 59.15% for TMD, type 1 far field, type 1 near field, type 1 far-near field, type 2 far field, type 2 near field, and type 2 far-near field, respectively.

The analysis and simulation indicate that type 2 FLC is more successful than type 1 FLC to reduce seismic responses of both bridges. Because reduction of responses of first and third spans of Vincent Thomas suspension with type 2 FLC in comparison to type 1 FLC for all earthquakes are 11.38%, 31.85%, and 21.42% and for second span are 8.51%, −8.99%, and 20.44% for optimal far-field, near-field, and far-near field controllers. Furthermore, reduction of responses of first and third spans of Golden Gate suspension bridge with type 2 FLC in comparison to type 1 FLC for all earthquakes are 15.50%, 21.76%, and 21.42% and for second span are 15.86%, 21.34%, and 20.44% for optimal far-field, near-field, and far-near field controllers. Hence, the results show that type 2 FLC which is optimized with near-field earthquakes has the best performance compared with other control systems to reduce seismic responses.

For instance, Figure 7 shows maximum responses of bridges node subjected to TCU129 earthquakes.

Part (a) of Figure 7 illustrates that when the fuzzy type 2 is adjusted to the far-field parameters to control the short spans suspension bridge subjected to near-field ground motions, the results will be undesirable while this inappropriate condition does not occur in long suspension bridge, but there is no extreme difference between type 2 and the other control systems. In addition, this is clearly seen that by increasing the span of bridges the performance of TMD is reduced. This fact can be justified by the increasing of the flexibility causing the more spaced modes. In addition, Figure 7 indicates that in short suspension bridge, ATMD which has fuzzy type 2 adjusted to the near or near-far field parameters as the controller provides the best results. But in long-span ones, both fuzzy type 1 and 2 make desirable response reduction; however, the best performance belongs to fuzzy type 2. Figure 8 illustrates peak energy for all controlled systems and uncontrolled bridges including Vincent Thomas and Golden Gate under two near and far-field earthquakes respectively. According to the figure, both fuzzy controllers have better performance to dissipate energy in comparison to uncontrolled bridges. Furthermore, fuzzy type 2 controllers are more slightly successful than fuzzy type 1 counterparts. Figure 9 demonstrates the variation of the maximum displacement in account to the peak ground acceleration (PGA) of the selected near-field ground motions records represented in Table 4. According to Figure 9, this is obvious that the maximum response does not raise by increasing the PGA. In addition, the curvature of FLC type 2 places

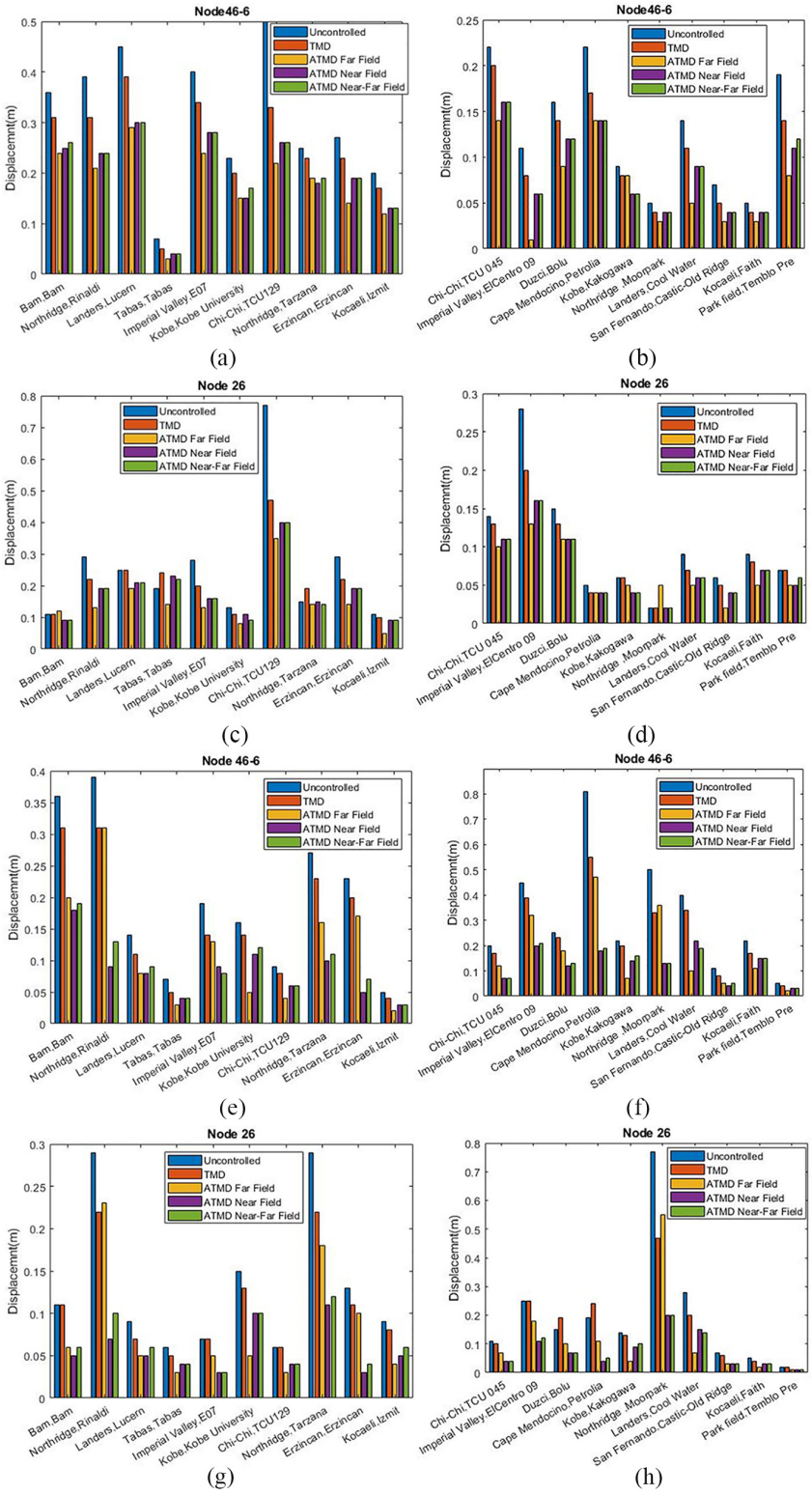


Figure 5. Maximum controlled displacement of Vincent Thomas suspension bridge controlled by type 1 and type 2 fuzzy controller system for each earthquake: (a) maximum displacement of node 46-6 under near-field earthquakes for type 1 controller; (b) maximum displacement of node 46-6 under far-field earthquakes for type 1 controller; (c) maximum displacement of node 26 under near-field earthquakes for type 1 controller; (d) maximum displacement of node 26 under far-field earthquakes for type 1 controller; (e) maximum displacement of node 46-6 under near-field earthquakes for type 2 controller; (f) maximum displacement of node 46-6 under far-field earthquakes for type 2 controller; (g) maximum displacement of node 26 under near-field earthquakes for type 2 controller; and (h) maximum displacement of node 26 under far-field earthquakes for type 2 controller.

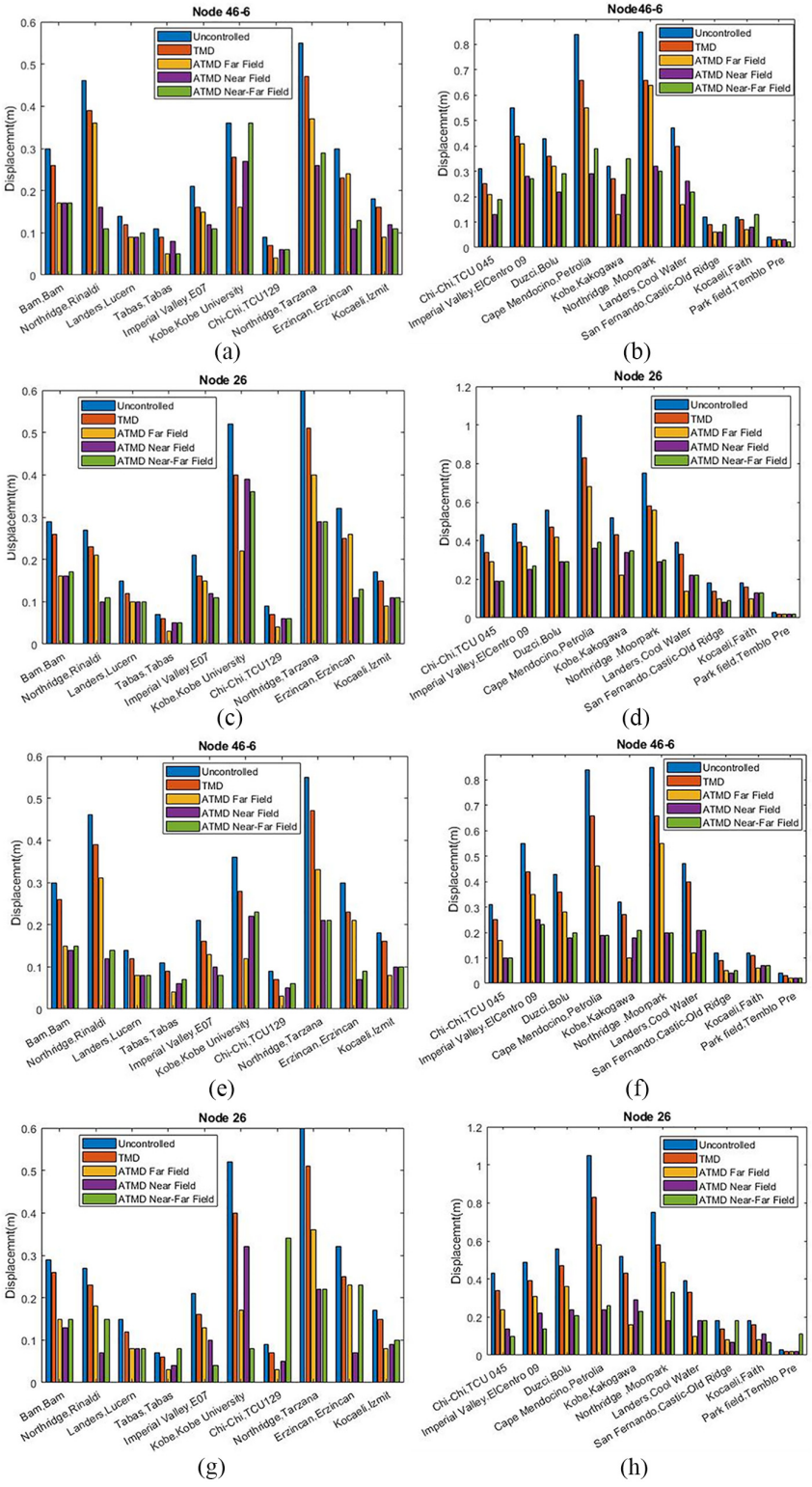


Figure 6. Maximum controlled displacement of Golden Gate suspension bridge controlled by type 1 and type 2 fuzzy controller system for each earthquake: (a) maximum displacement of node 46-6 under near-field earthquakes for type 1 controller; (b) maximum displacement of node 46-6 under far-field earthquakes for type 1 controller; (c) maximum displacement of node 26 under near-field earthquakes for type 1 controller; (d) maximum displacement of node 26 under far-field earthquakes for type 1 controller; (e) maximum displacement of node 46-6 under near-field earthquakes for type 2 controller; (f) maximum displacement of node 46-6 under far-field earthquakes for type 2 controller; (g) maximum displacement of node 26 under near-field earthquakes for type 2 controller; and (h) maximum displacement of node 26 under far-field earthquakes for type 2 controller.

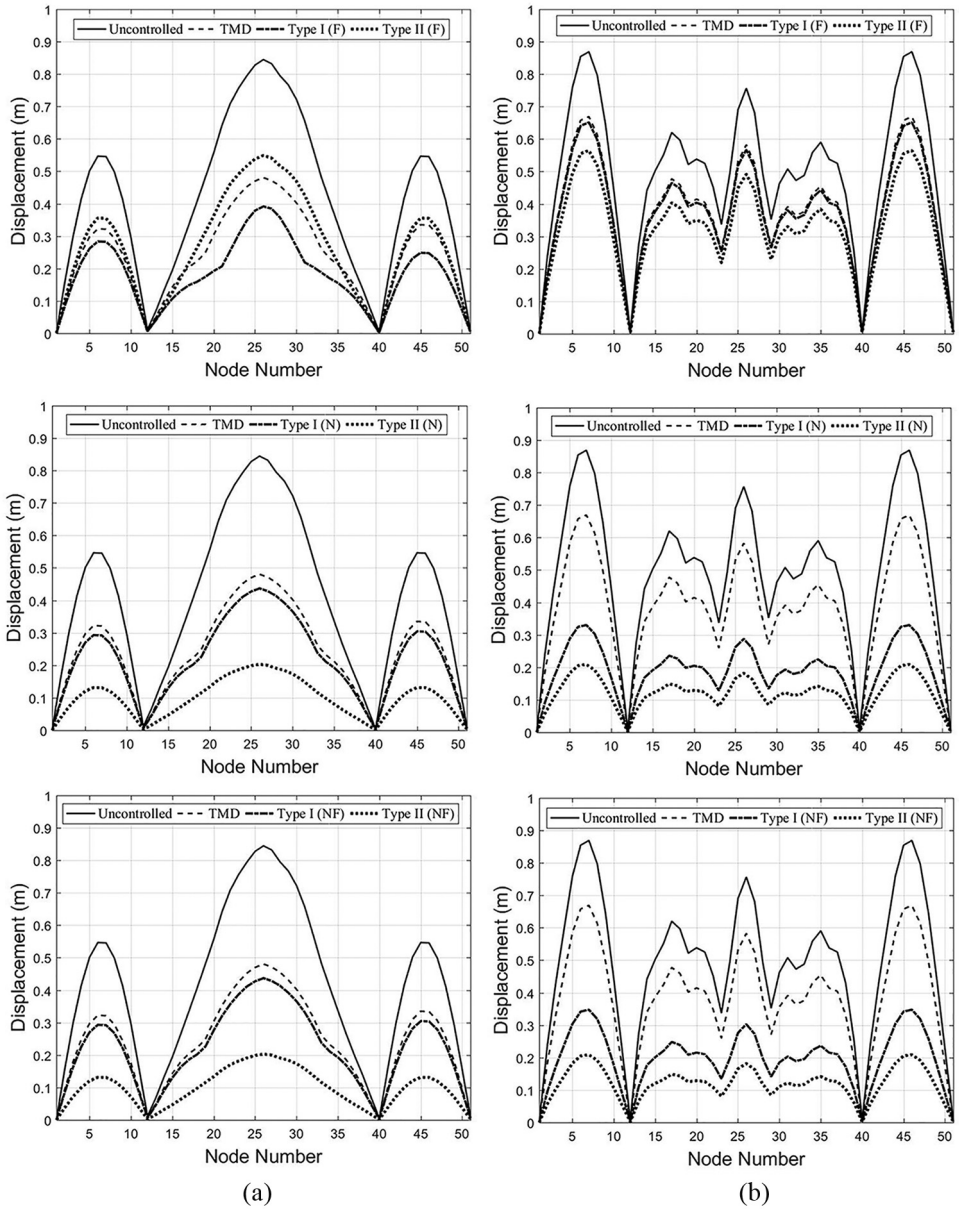


Figure 7. Maximum responses of bridges node subjected to TCU129 earthquakes: (a) Vincent Thomas and (b) Golden Gate.

bottom of the all curvatures which indicates the maximum response reduction and best performance of it while TMD and FLC type 1 in some ground motions records increase the final response in comparison to uncontrolled condition. Also, both ATMD systems including FLC type 1 and 2 provide better response reduction in higher PGAs such that maximum response reduction is corresponded to the highest PGA.

Conclusion

The performance of TMD and ATMD were investigated in the short and long-span suspension bridges. Two different FLCs including type 1 and type 2 FLCs were used to control the suspension bridges. TMD's parameters and ATMD's FLCs were optimized by LPOA algorithm as a meta-heuristic one. The Vincent Thomas suspension and Golden Gate bridges were chosen for numerical analysis, equipped by six different ATMD systems based on sensitivity to near and far-field ground motions. Then, the bridges are subjected to 20 different earthquakes, and the responses of bridges in different optimal control systems including passive and active ones were compared to uncontrolled condition. The seismic responses of bridge are reduced between 12%-39% or TMD, and 21%-79% for all

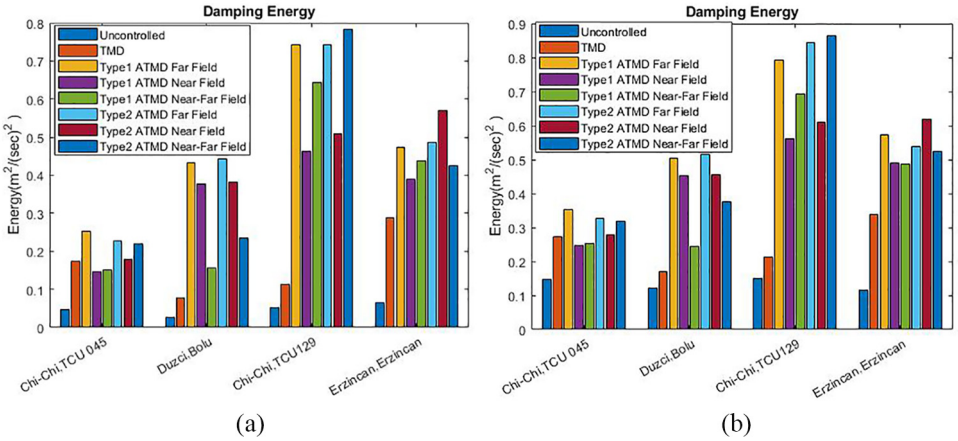


Figure 8. Peak dissipated energy for the uncontrolled and controlled Vincent Thomas and Golden Gate Bridges: (a) damping energy for Vincent Thomas and (b) damping energy for Golden Gate.

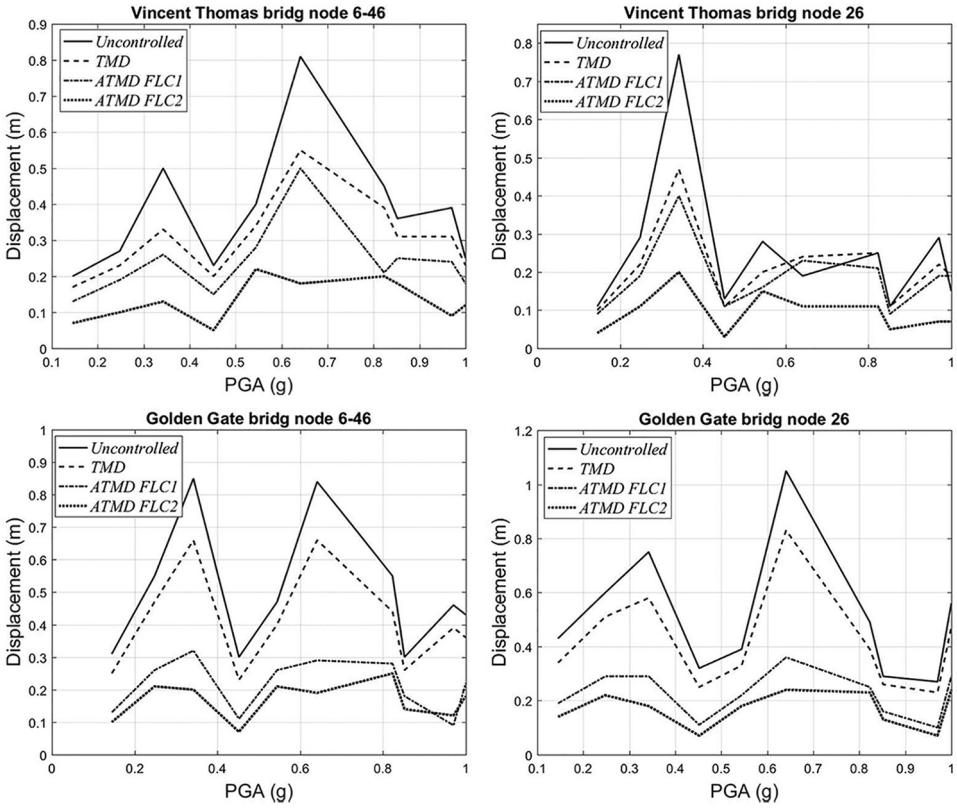


Figure 9. Behavior of response reduction in account to PGA.

optimized ATMD systems compared with the uncontrolled one. The most important results are listed as follows:

1. By increasing the length of the span, more spaced modes are appeared causing the performance decrement of TMD and increasing the efficiency of ATMD controlled by fuzzy type 1 and type 2. Also, type 2 FLC has the better performance than type 1 FLC.
2. For the short-span suspension bridge, type 1 fuzzy and type 2 fuzzy optimized according to the far-field and near-field condition respectively provide the most effective results. In

addition, for long-span ones near-field condition is optimum for type 1 and type 2.

3. In long and short-span suspension bridges, type 2 fuzzy provides the better performance in comparison to type 1. However, the difference of performance in short suspension bridge is low and is obvious in long-span ones. For the short-span suspension bridge located far from the fault, the ATMD system that its type 2 fuzzy controller adjusted to the far-field parameters provides the best performance while for the bridge near to the fault the parameters of near or near-far field condition can be used. For long-span ones, last definition is acceptable when near-field parameters are used for near fault region.
4. Even though maximum response does not necessarily increase by raising the PGA, maximum response reduction will be increased by rising PGA in both ATMD systems.
5. Both ATMD systems (type 1 and type 2) are slightly successful to dissipate energy in comparison to TMD and uncontrolled bridges.

Declaration of Conflicting Interests

The author(s) declared no potential conflicts of interest with respect to the research, authorship, and/or publication of this article.

Funding

The author(s) received no financial support for the research, authorship, and/or publication of this article.

ORCID iD

Seyed Hossein Hosseini Lavasani https://orcid.org/0000-0002-9524-9399

References

Abdel-Ghaffar AM (1980) Vertical vibration analysis of suspension bridges. *Journal of Structural Division* 106(10): 2053–2075.

Abdel-Ghaffar AM and Rubin LI (1983) Lateral earthquake response of suspension bridges. *Journal of Structural Engineering* 109(3): 664–675.

Amini F and Doroudi R (2010) Control of a building complex with magneto-rheological dampers and tuned mass damper. *Structural Engineering and Mechanics* 36(2): 181–195.

Bathaei A, Ramezani M and Ghorbani-TanhaA (2017) Type-1 and type-2 fuzzy logic control algorithms for semi-active seismic vibration control of the college urban bridge using MR dampers. *Civil Engineering Infrastructures Journal* 50(2): 333–351.

Carpineto N, Lacarbonara W and Vestroni F (2010) Mitigation of pedestrian-induced vibrations in suspension footbridges via multiple tuned mass dampers. *Journal of Vibration and Control* 16(5): 749–776.

Castillo O and Melin P (2008) *Type-2 Fuzzy Logic: Theory and Applications*. Berlin, Heidelberg: Springer-Verlag.

Chen H, Sun Z and Sun L (2011) Active mass damper control for cable stayed bridge under construction: an experimental study. *Structural Engineering and Mechanics* 38(2): 141–156.

Clough RW and Penzien J (2010) *Dynamics of Structures*. Berkeley, CA: Computers and Structures, Inc.

Debbarma R and Das D (2016) Vibration control of building using multiple tuned mass dampers considering real earthquake time history. *International Journal of Civil and Environmental Engineering* 10(6): 694–704.

Elias S (2018) Seismic energy assessment of buildings with tuned vibration absorbers. *Shock and Vibration* 2018: 2051687.

Elias S and Matsagar V (2017a) Effectiveness of tuned mass dampers in seismic response control of isolated bridges including soil-structure interaction. *Latin American Journal of Solids and Structures* 14(13): 2324–2341.

Elias S and Matsagar V (2017b) Passive-hybrid system of base-isolated bridge with tuned mass absorbers. In: Rupakhety R, Olafsson S and Bessason B (eds) *Proceedings of the International Conference on Earthquake Engineering and Structural Dynamics*. Cham: Springer, pp. 95–109.

Elias S and Matsagar V (2017c) Research developments in vibration control of structures using passive tuned mass dampers. *Annual Reviews in Control* 44: 129–156.

Hossein Lavassani SH, Alizadeh H and Homami P (2020) Optimizing tuned mass damper parameters to mitigate the torsional vibration of a suspension bridge under pulse-type ground motion: A sensitivity analysis. *Journal of Vibration and Control* 26(11–12): 1054–1067.

Huang MH, Thambiratnam DP and Perera NJ (2005) Vibration characteristics of shallow suspension bridge with pretensioned cables. *Engineering Structures* 27(8): 1220–1233.

Kaveh A and Mahjoubi S (2018) Lion pride optimization algorithm: a meta-heuristic method for global optimization problems. *Scientia Iranica* 25(6B): 3113–3132.

Larsena A, Svensson E and Andersen H (1995) Design aspects of tuned mass dampers for the Great Belt East Bridge approach spans. *Journal of Wind Engineering and Industrial Aerodynamics* 54–55(C): 413–426.

Ling X and Zhang Y (2011) Operations on triangle type-2 fuzzy sets. *Procedia Engineering* 15: 3346–3350.

Matin A, Elias S and Matsagar V (2020) Distributed multiple tuned mass dampers for seismic response control in bridges. *Proceedings of the Institution of Civil Engineers—Structures and Buildings* 173(3): 217–234.

Nikkhoo A, Eskandari AB, Farazandeh A, et al. (2019) Vibration control of bridges under simultaneous effects of earthquake and moving loads using steel pipe dampers. *Journal of Vibration and Control* 25(19–20): 2580–2594.

Pourzeynali S and Datta TK (2005) Semiactive fuzzy logic control of suspension bridge flutter. *Journal of Structural Engineering* 131(6): 900–912.

Pourzeynali S and Esteki S (2009) Optimization of the TMD parameters to suppress the vertical vibration of the suspension bridges subjected to earthquake excitation. *International Journal of Engineering, Transactions B: Applications* 22(1): 23–34.

Pourzeynali S, Lavasani HH and Modarayi AH (2007) Active control of high rise building structures using fuzzy logic and genetic algorithms. *Engineering Structures* 29(3): 346–357.

Ross TJ (2010) *Fuzzy Logic with Engineering Applications*. 3rd ed. West Sussex: John Wiley & Sons.

Siddique N and Adeli H (2013) *Computational Intelligence: Synergies of Fuzzy Logic, Neural Networks and Evolutionary Computing*. Hoboken, NJ: Wiley.

Tanida K (2002) Progress in the application of active vibration control technologies to long-span bridges in Japan. *Progress in Structural Engineering and Materials* 4(4): 363–371.

Wang H, Tao T, Cheng H, et al. (2014) Simulation study on train-induced vibration control of a long-span steel truss girder bridge by tuned mass dampers. *Mathematical Problems in Engineering* 2014: 506578.

Wen YK and Sun LM (2015) Distributed ATMD for buffeting control of cable-stayed bridges under construction. *International Journal of Structural Stability and Dynamics* 15(3): 1450054.